Project 31451: Subproject “Upwelling”

Results after 1 year's activity

Werner Alpers

University of Hamburg, Hamburg, Germany

DanLing Tang

South China Sea Institute of Oceanology, Guangzhou, China

In the last year we have addressed the following issues:

- Radar signatures of biogenic surface films and mineral oil films
- Radar, optical, and infrared signatures of upwelling regions and of sea areas hit by typhoons
- Relationship between Chl-a distribution patterns and ocean currents
- Effect of typhoons on CO2 fluxes across the air-sea interface
- Effect of upwelling on the distribution of phytoplankton size structure
- The response of the mixed layer depth to tropical cyclones

➢Radar signatures of biogenic surface films and mineral oil films

It is not straightforward to determine unambiguously whether dark patches originate from mineral oil films or from biogenic slicks.

A paper has been submitted to “Remote Sensing of Environment” with the title:
“Oil spill detection by imaging radars: challenges and pitfalls”.
by Werner Alpers, Benjamin Holt and Kan Zeng.

One result: Radar backscattering from mineral oil films as well as from biogenic slicks (monomolecular surface films) can be described by Bragg scattering theory.

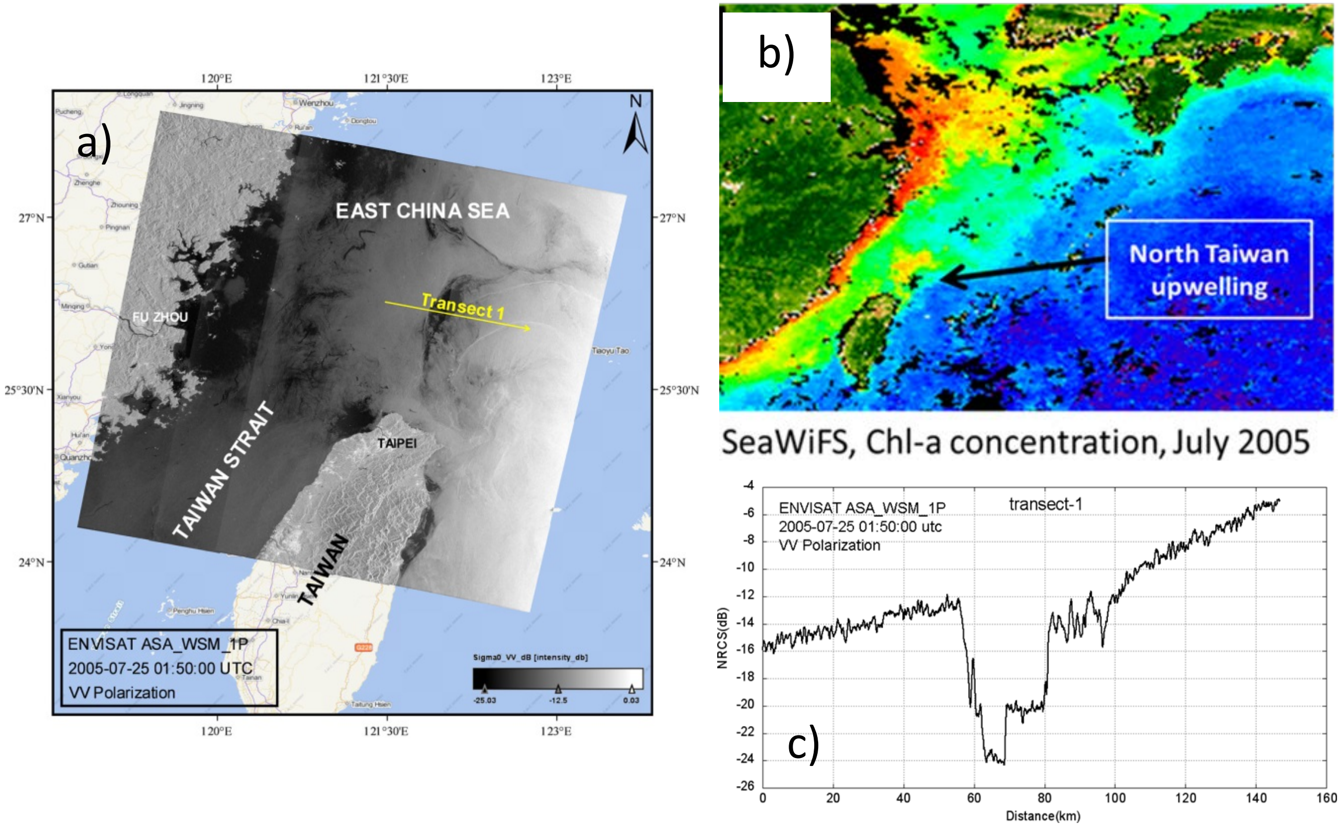

(a) Envisat ASAR image acquired in the Wide Swath (WS) mode (swath width: 400 km) on 25 July 2005 at 01:54 UTC over the southern East China Sea. Visible is in the lower central section the island of Taiwan. The dark patch north of Taiwan and the dark band along the east coast of China are very likely caused by biogenic slicks. (b) Chl-a concentration in July 2005 retrieved from SeaWiFS data showing enhanced Chl-a concentration in an area north of Taiwan and along the east coast of China. These areas correlate well with the dark areas visible on the ASAR image which suggests that the dark areas are caused predominantly by biogenic slicks. (c) Plot of the NRCS along the transect inserted in Panel (a)

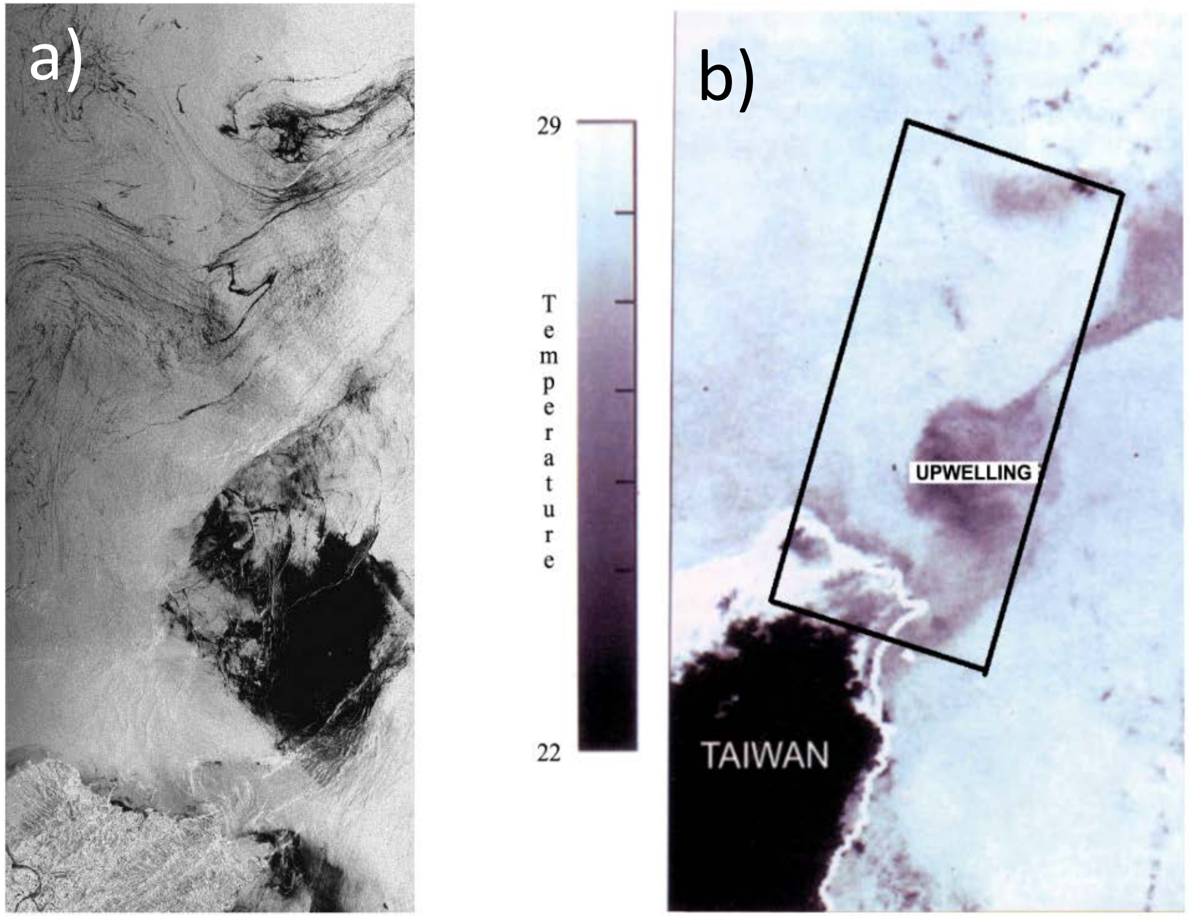

a) ERS-1 SAR image acquired on 23 July 1994 at 02:26 UTC over the upwelling area north of Taiwan. b) SST image (in degrees C) acquired by the AVHRR aboard the NOAA-11 satellite on 22 July 1994 at 08:03 UTC showing the upwelling area as an area of low SST. Source: Clemente-Colon (2005).

In upwelling regions, the reduction of the radar backscatter (NRCS) can be caused by

1. the damping of the short surface waves (responsible for the radar backscattering）by biogenic slicks.
2. the change of the stability of the air-sea interface from neutrally stable to stable (due to the cool upwelling water) or

Dependence of the C-band NRCS on the air-sea temperature difference

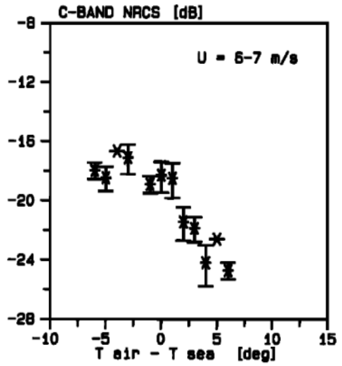

Fig. 6*a*. C band NRCS versus air-sea temperature difference for wind speeds between 6 and 7 m/s. The wind direction is between 125°N and 135°N. The number of data points is 136.

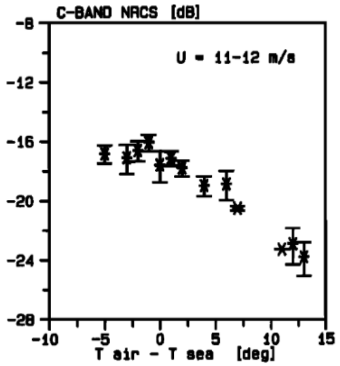

Fig. 6*c*. Same as Figure 6*a* but for wind speeds between 11 and 12 m/s and wind direction between 145°N and 155°N. The number of data points is 47.

From: Keller, Wismann, Alpers, JGR, 1989

➢Radar, optical, and infrared signatures of upwelling regions and of sea areas hit by typhoons

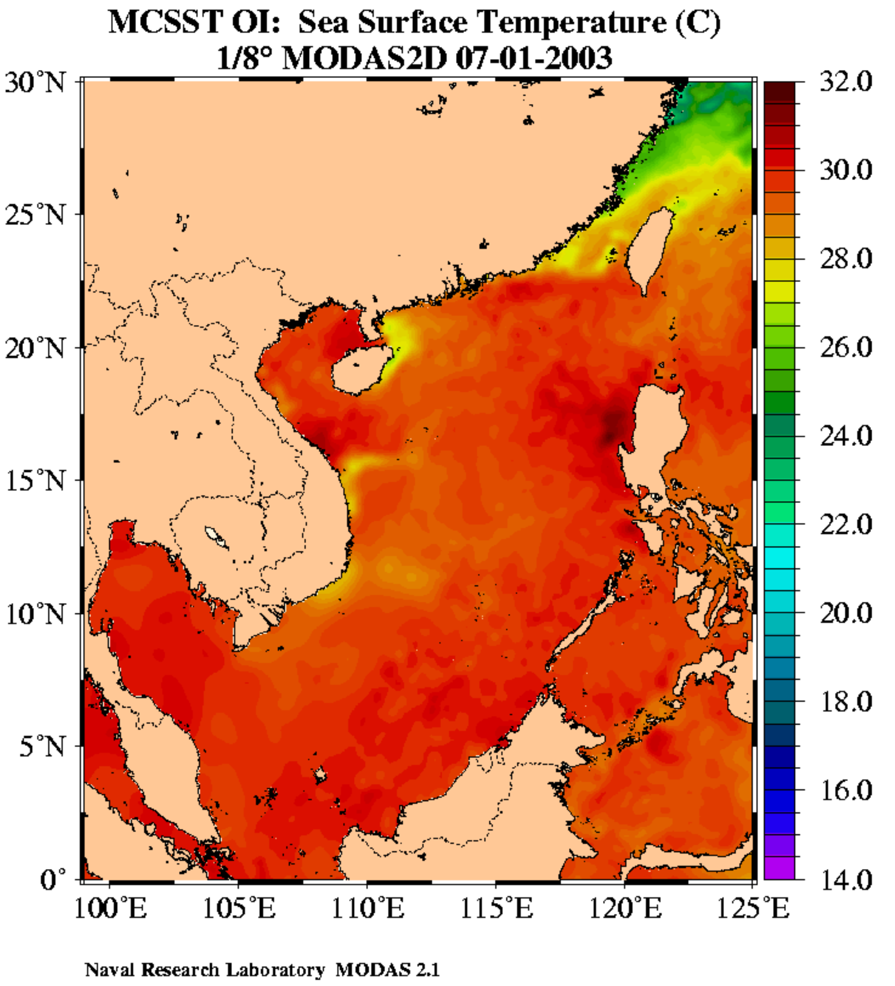

Sea Surface Temperature in June 2003 showing upwelling regions in the South China Sea and southern East China Sea

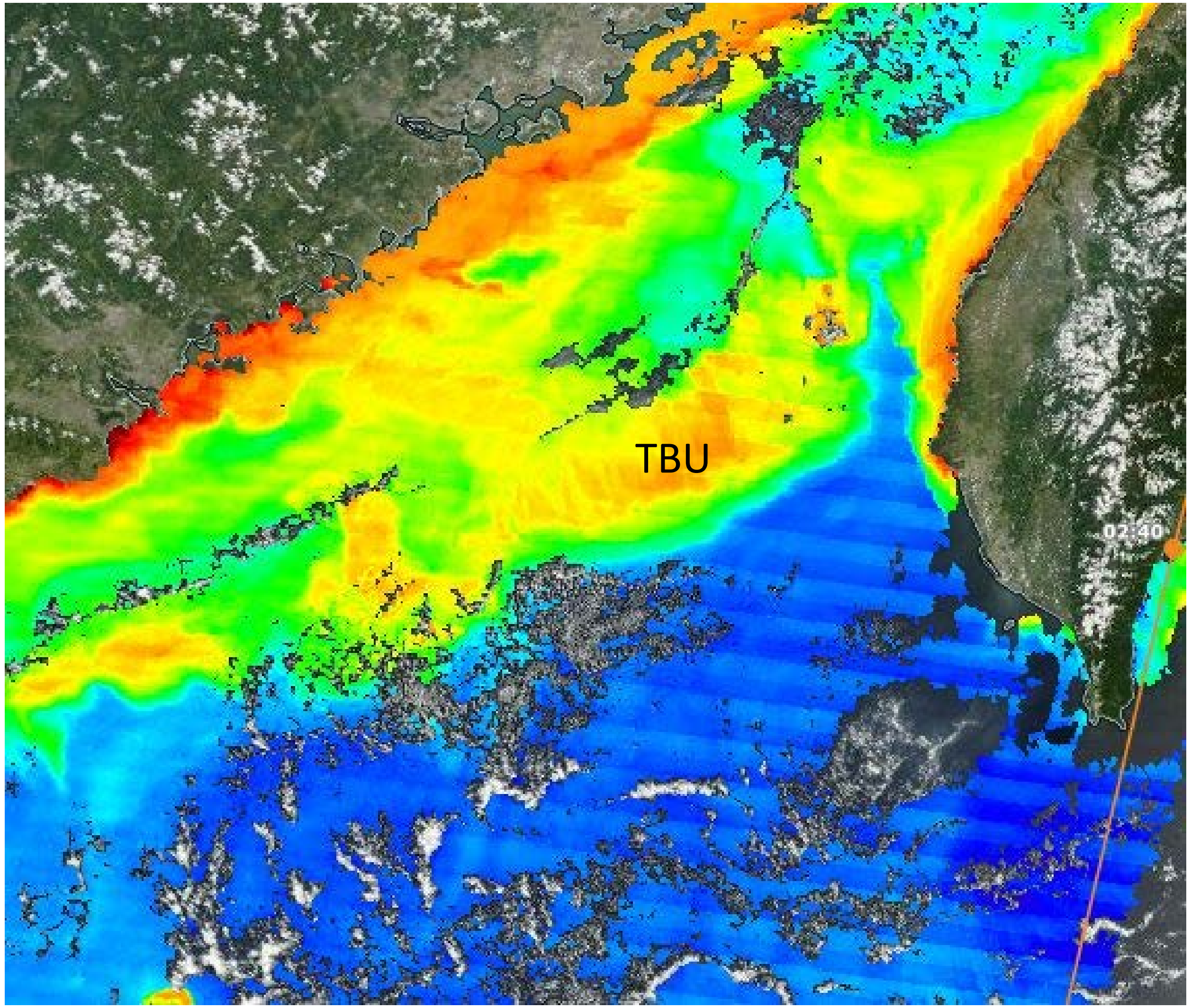

Chl-a, 4 August 2005, Terra/Aqua

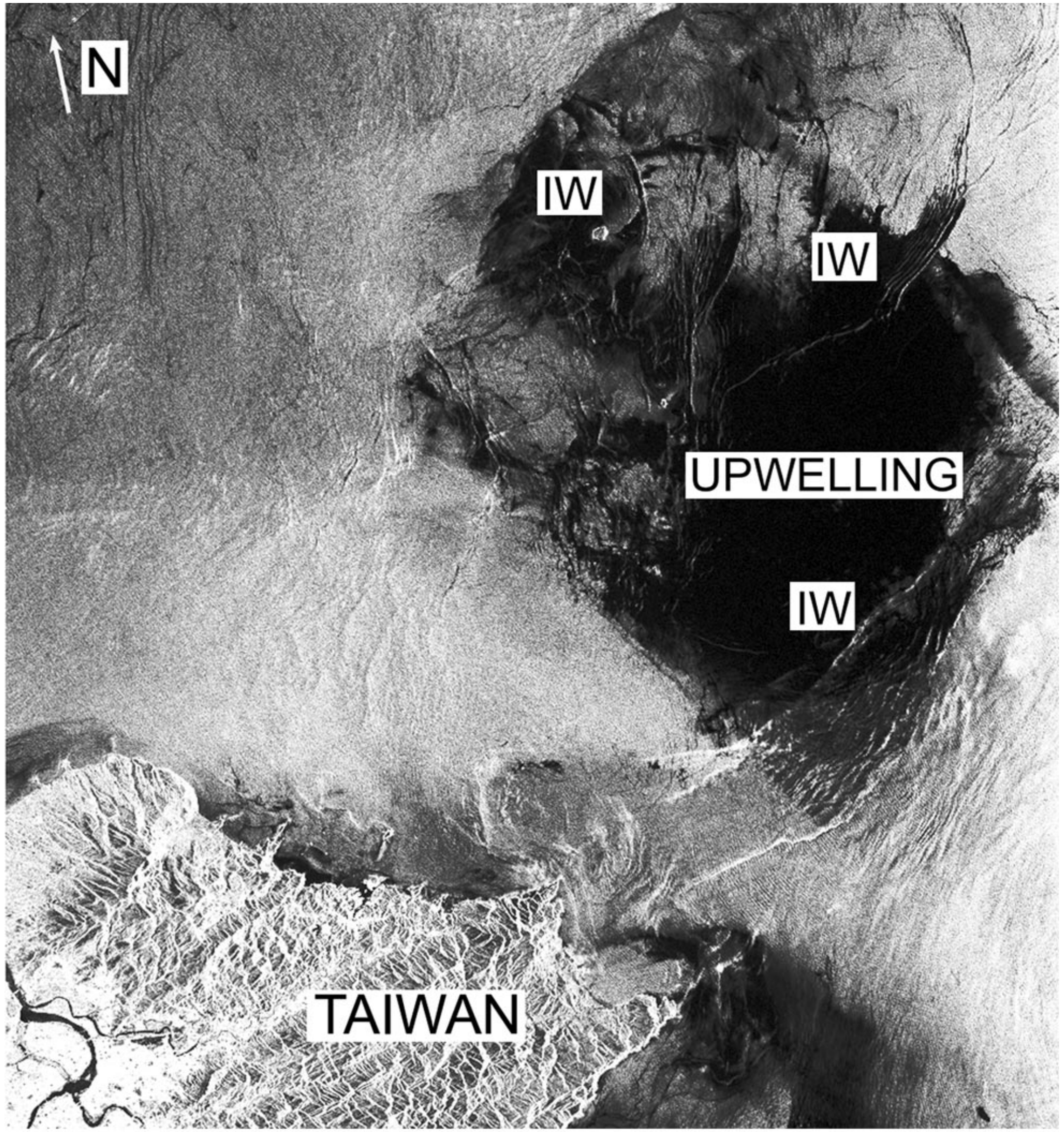

(a)

Upwelling area and packets of internal waves northeast of Taiwan on ERS-1 SAR image taken on 23 July 1994 at 02:26 UTC

Hsu, M.K., Mitnik, L.M., Liu, C.T., Upwelling area northeast of Taiwan on ERS-1 SAR images. *Acta Oceanographica Taiwanica* 1995. 34, 27-38.

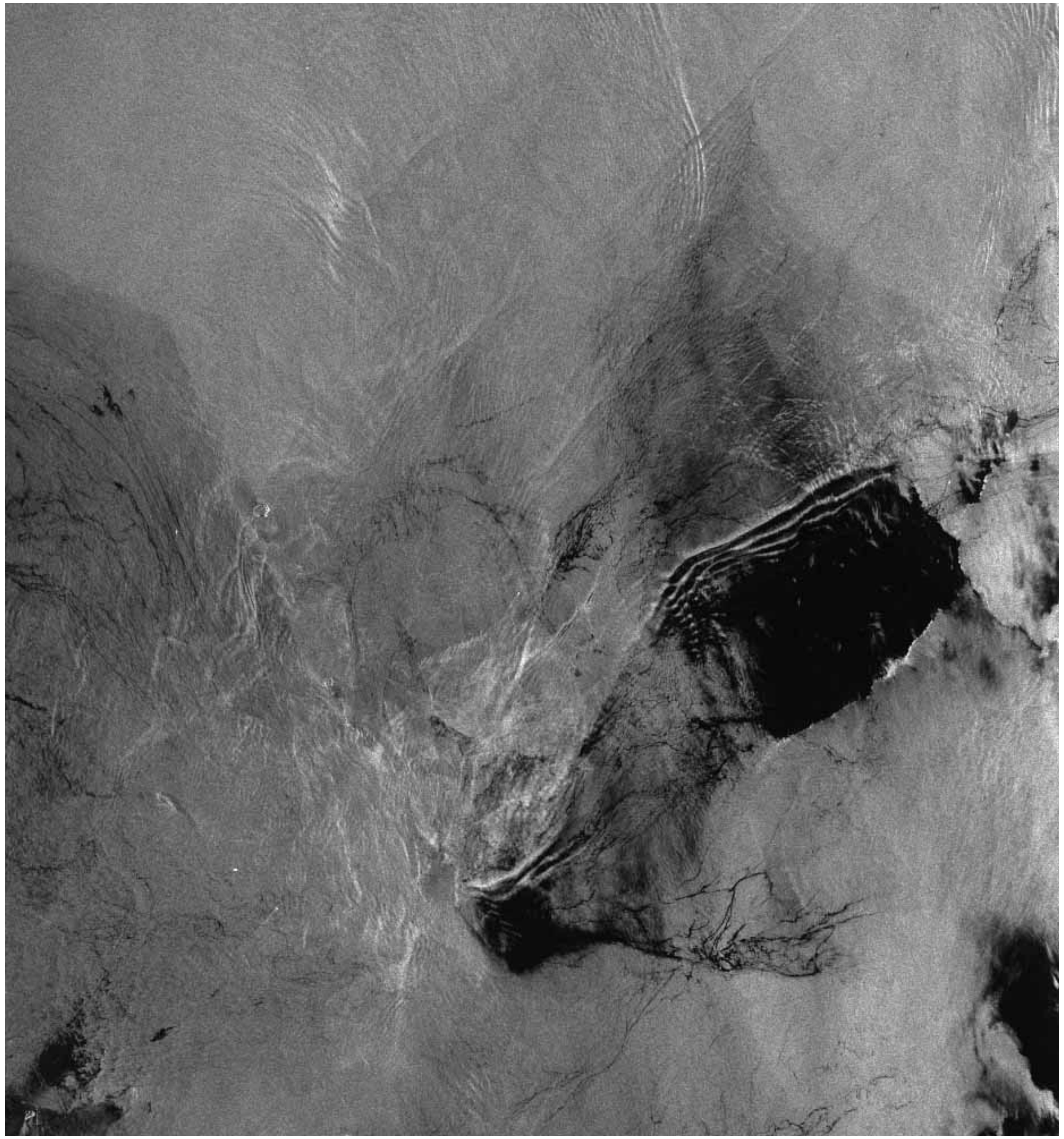

ERS-1 SAR
6 August 1995, 02:25 UTC

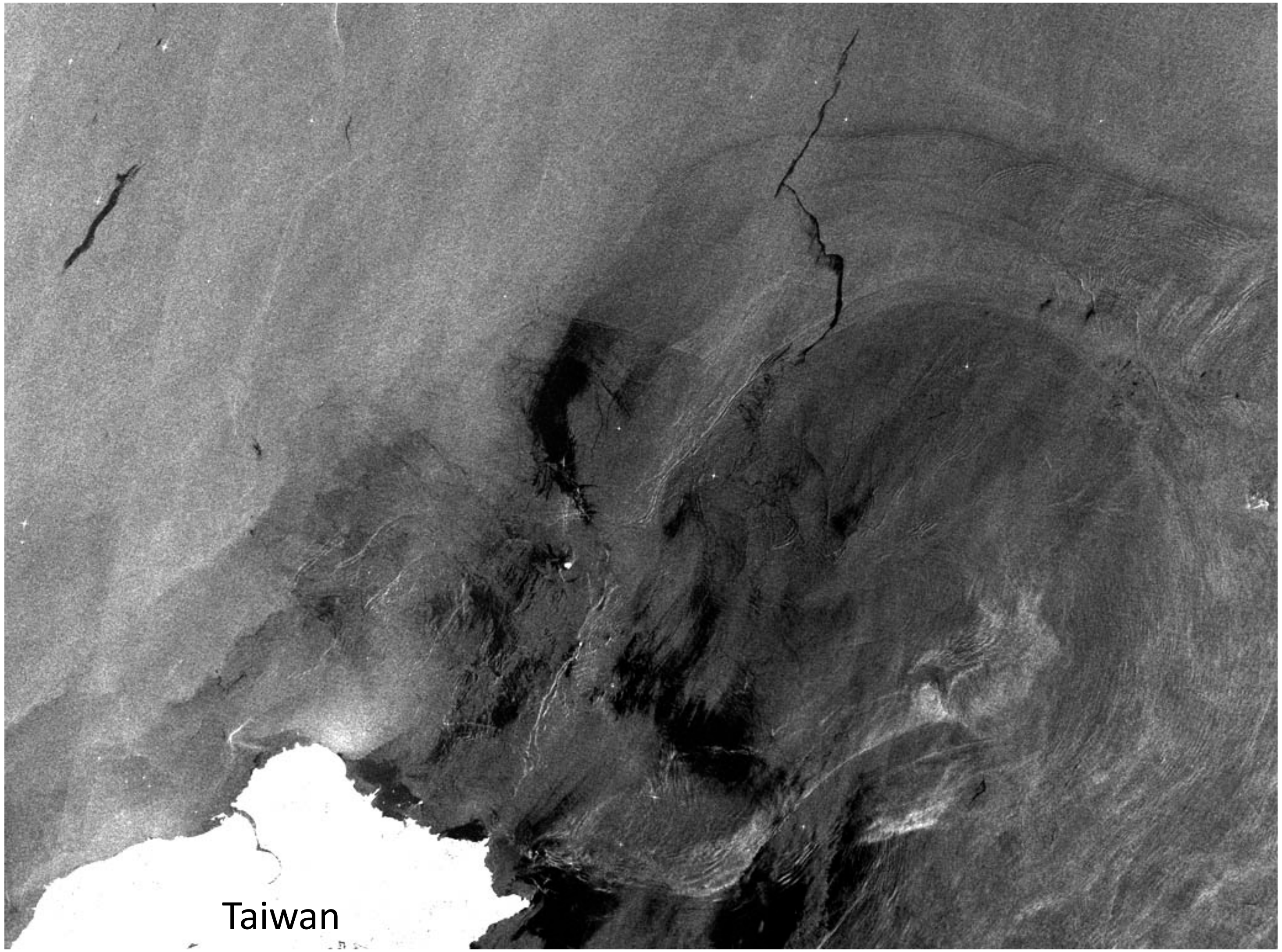

Envisat ASAR
31 August 2007,
0149 UTC

Typhoon Soudelor

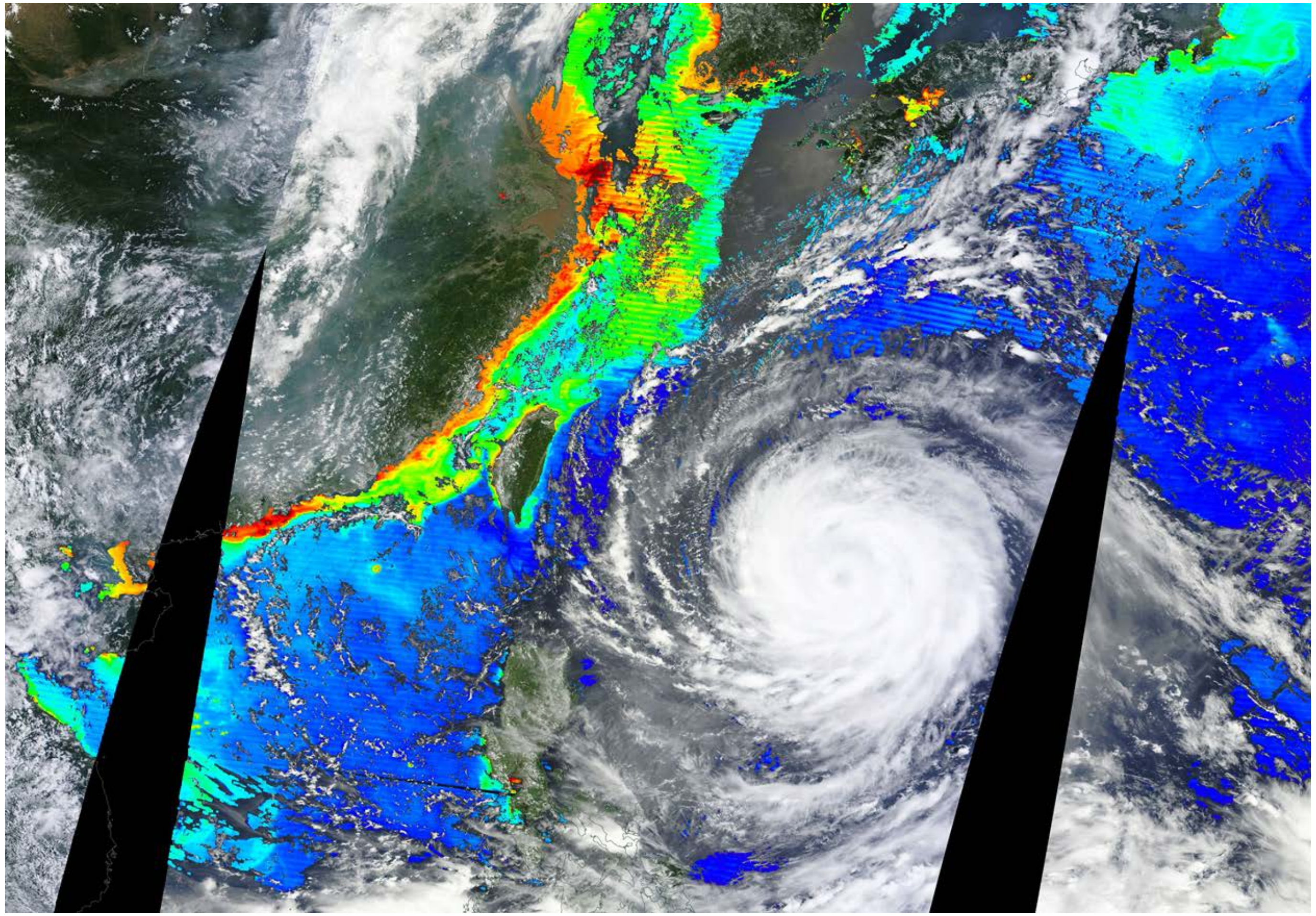

Cloud image (background) and Chl-a distribution , 6 August 2015
(source: Worldview)

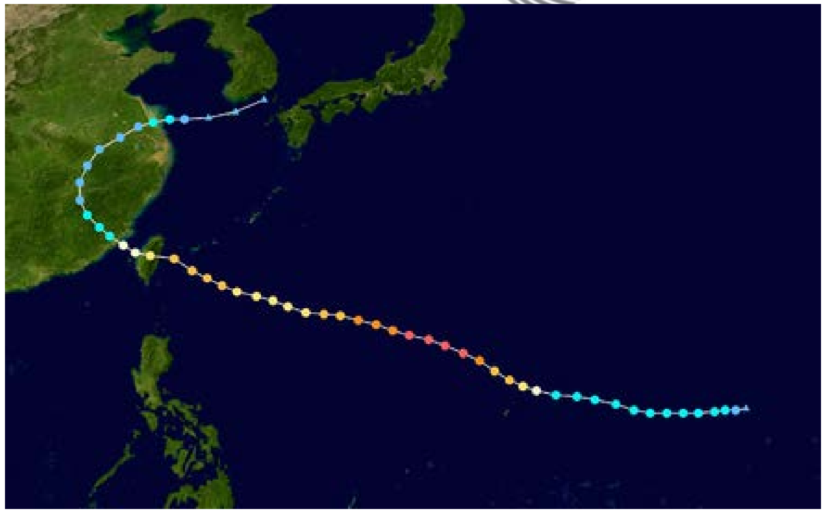

Formed: July 29, 2015
Dissipated: August 12, 2015
(Extratropical after August 11)
Highest winds: 10-minute sustained: 215 km/h (130 mph)
1-minute sustained: 285 km/h (180 mph)
Lowest pressure: 900 hPa (mbar); 26.58 inHg

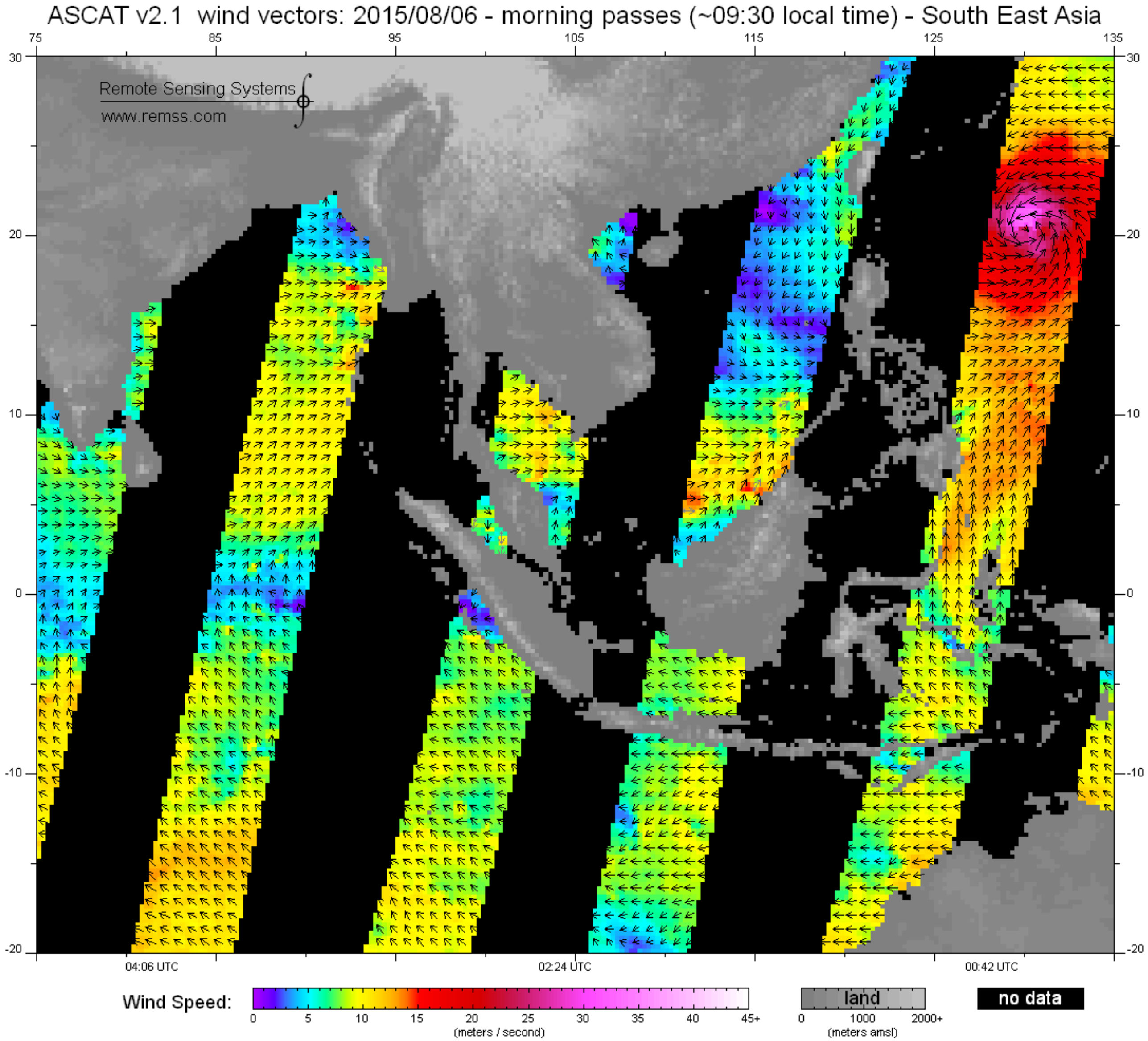

6 August 2005

6 days later

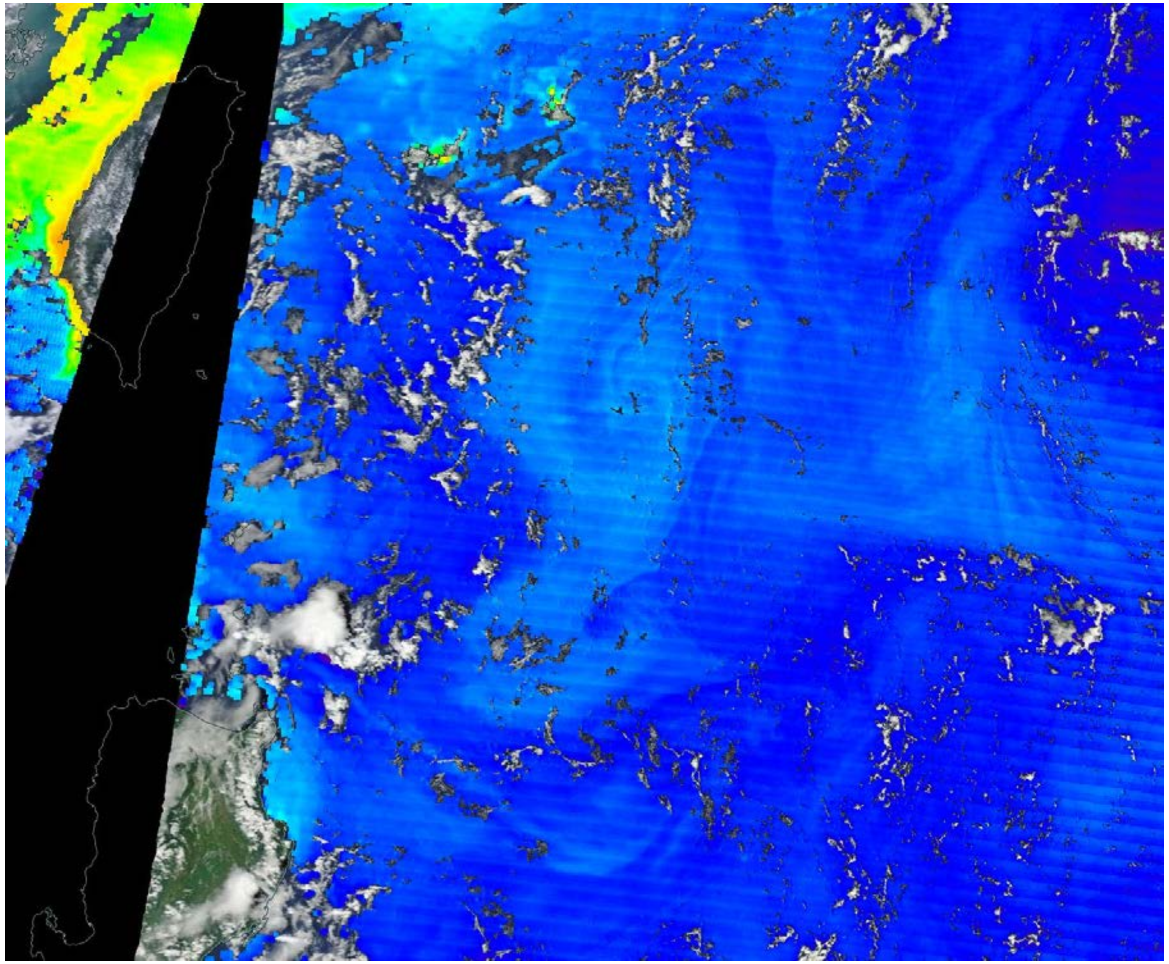

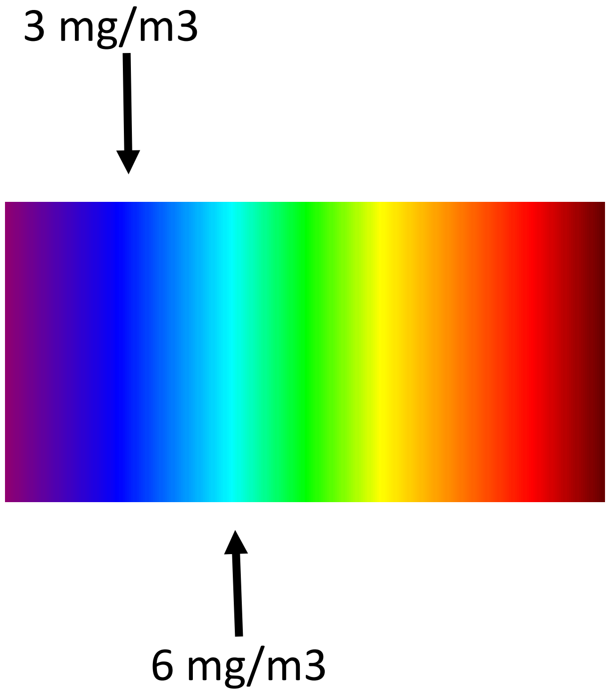

Chl-a distribution, 12 August 2015,

Typhoon Megi

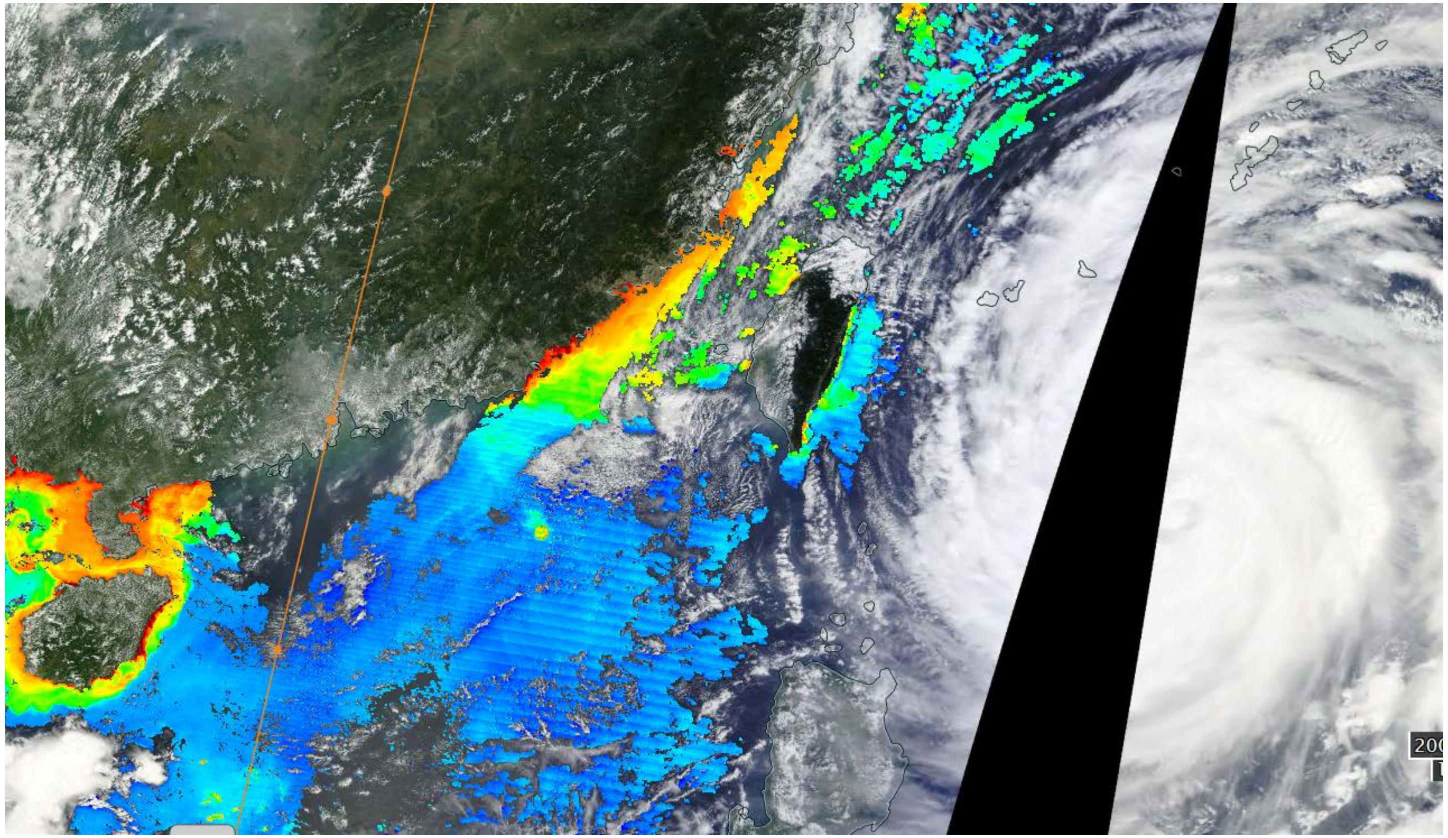

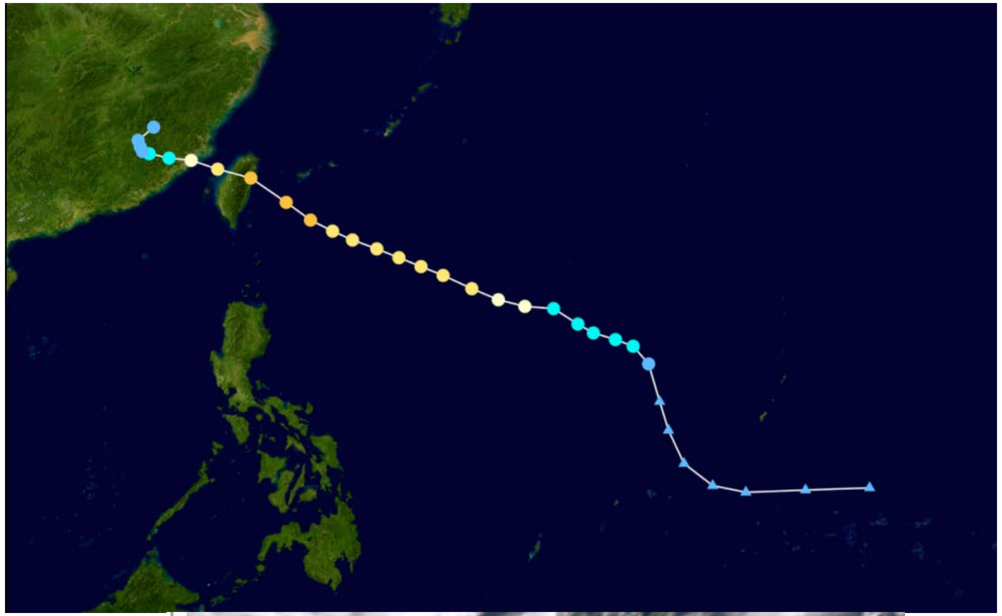

Typhoon Megi making landfall over Taiwan at peak intensity on September 27

Formed	September 22, 2016
Dissipated	September 29, 2016
Highest winds	*10-minute sustained:* 155 km/h (100 mph) *1-minute sustained:* 220 km/h (140 mph)
Lowest pressure	945 hPa (mbar); 27.91 inHg

SST and wind vector

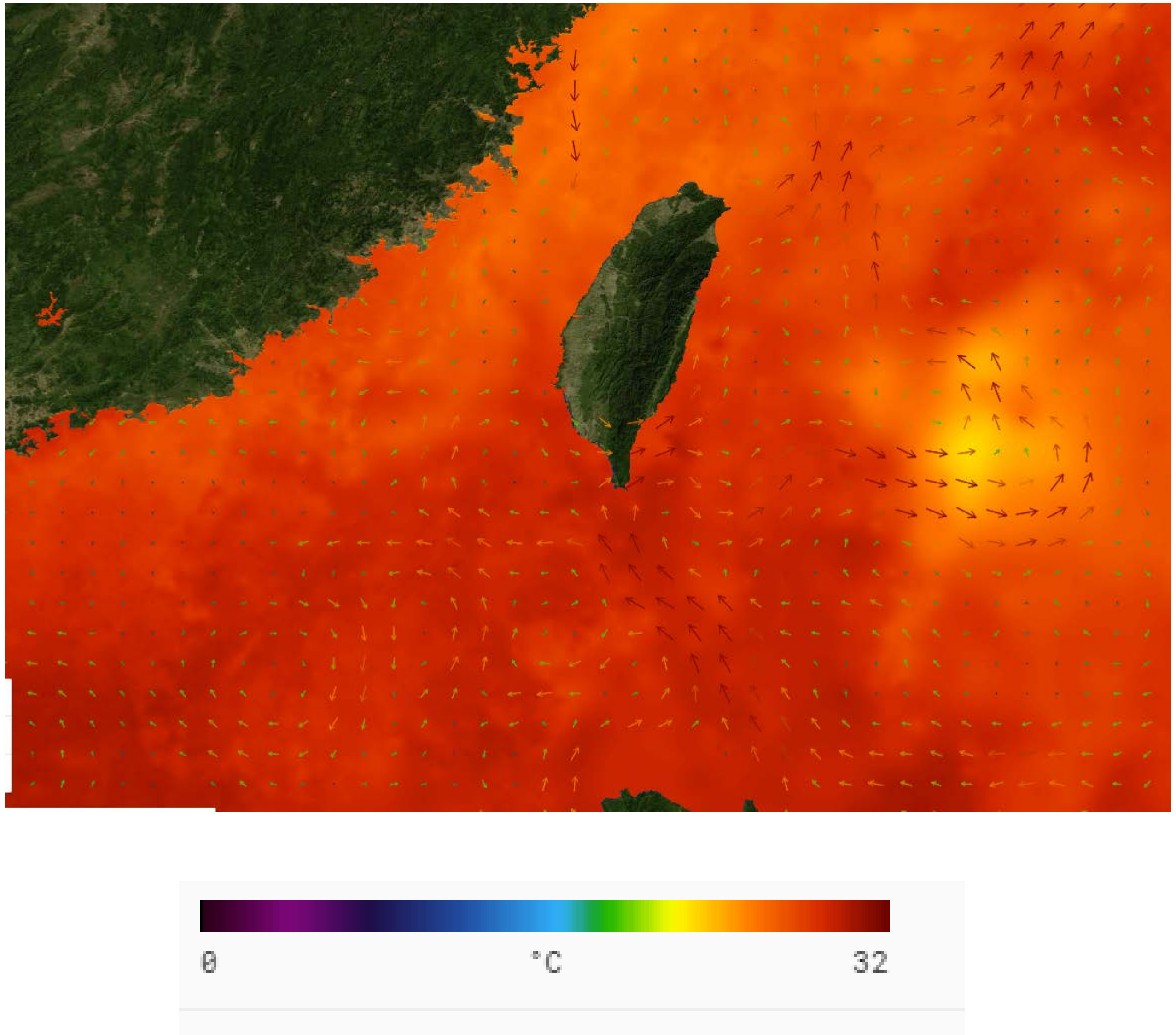

26 September 2016

➢ Relationship between Chl-a distribution patterns and ocean currents

Recurrent chl-a pattern north of Taiwan (from MODIS)

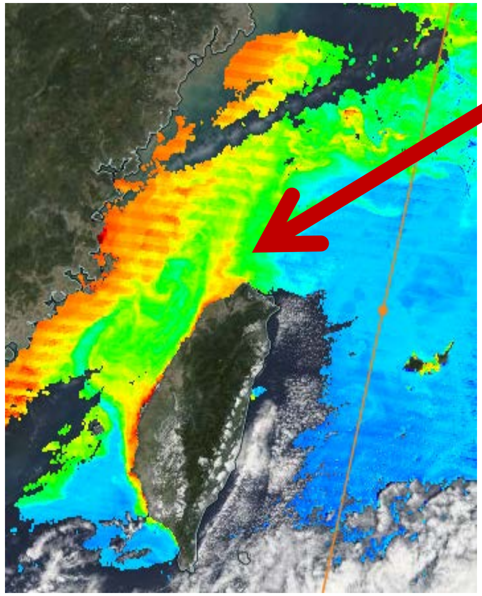

27 March 2017

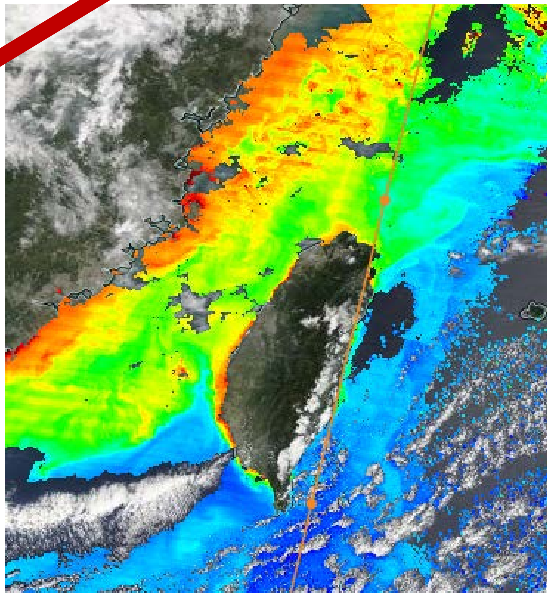

3 April 2017

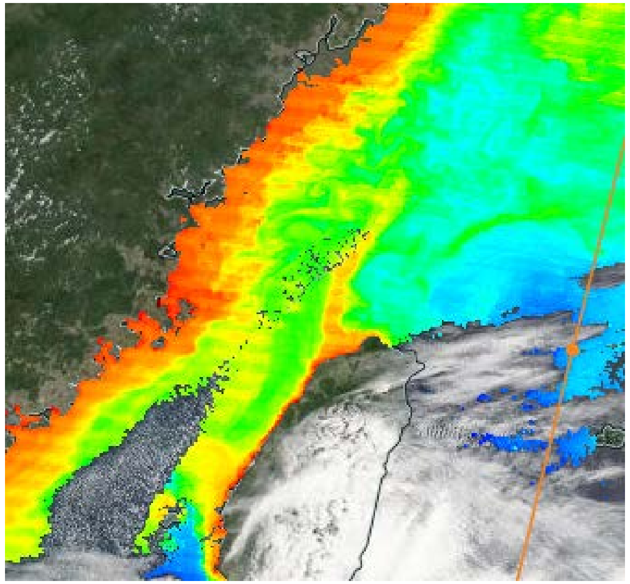

28 April 2017

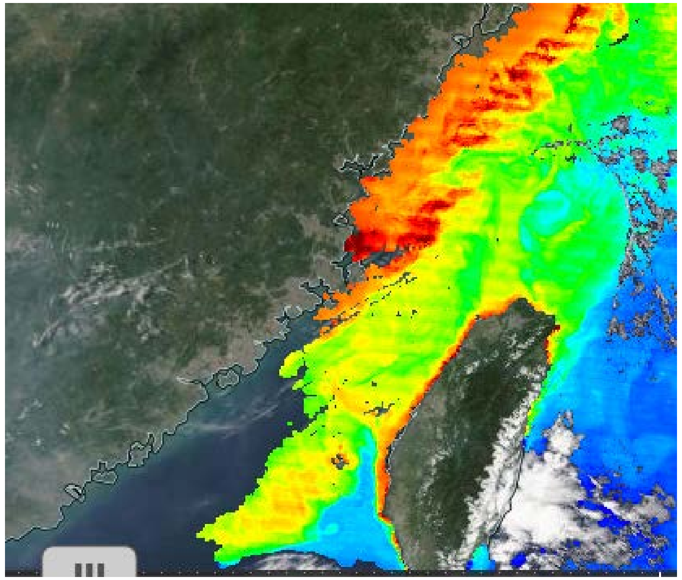

30 April 2017

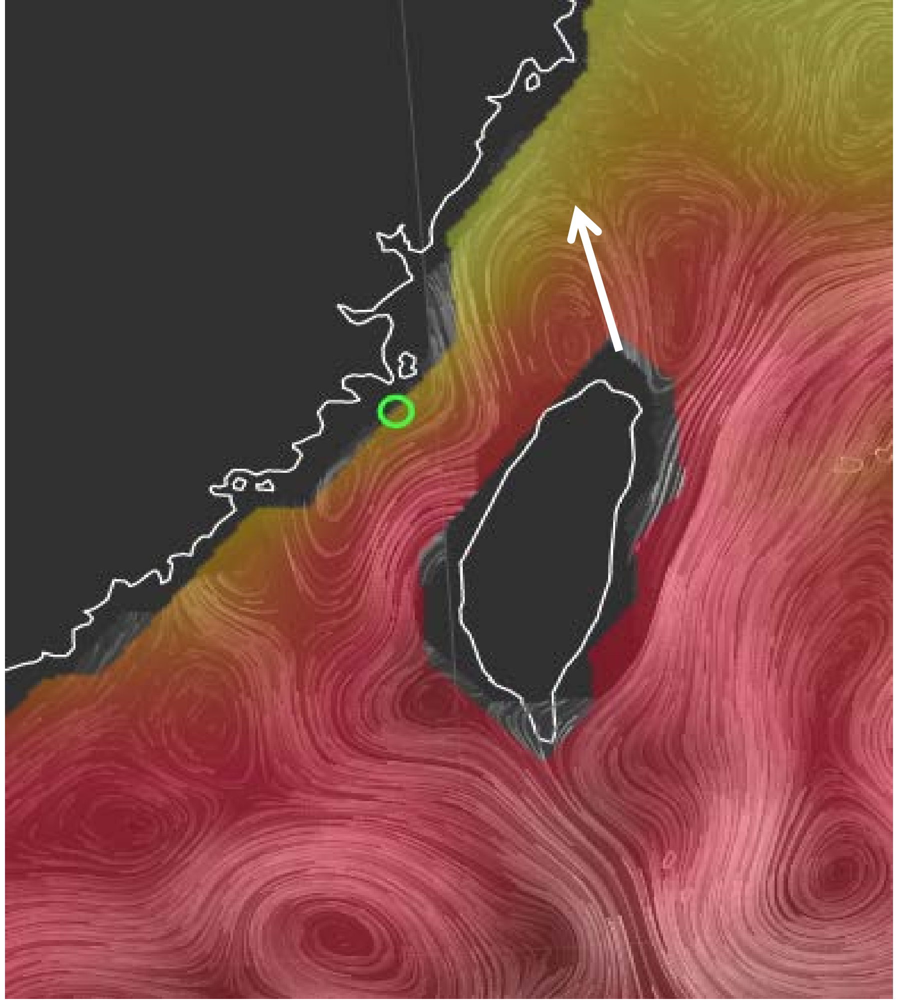

SST + NCEP currents,
28 April 2017

Time series of Chl-a pattern originating from the Pearl River

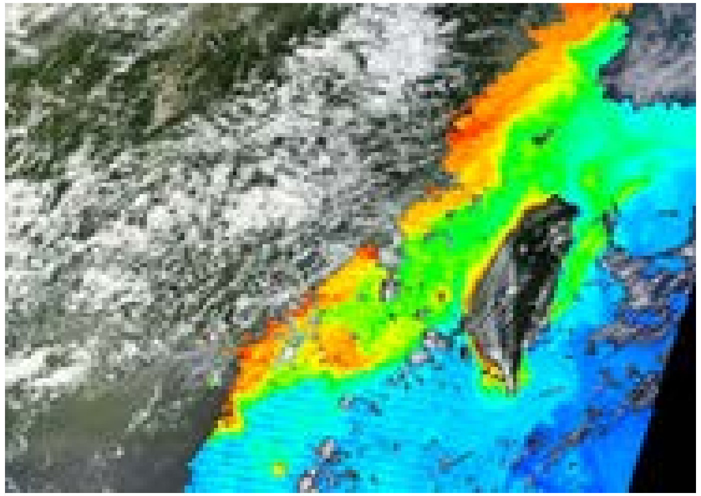

15 July 2016

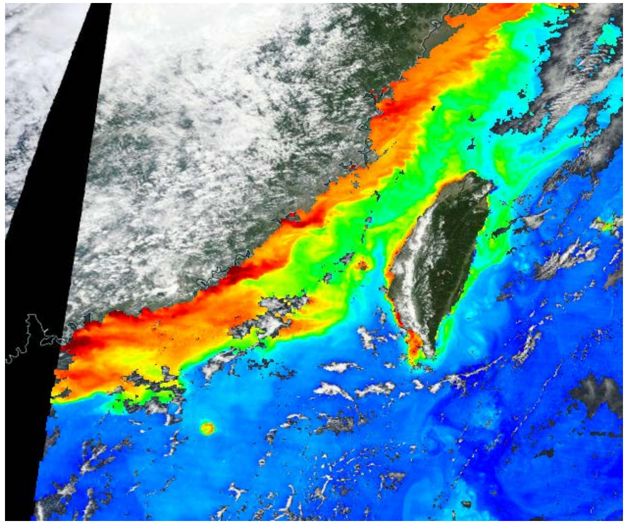

16 July 2016

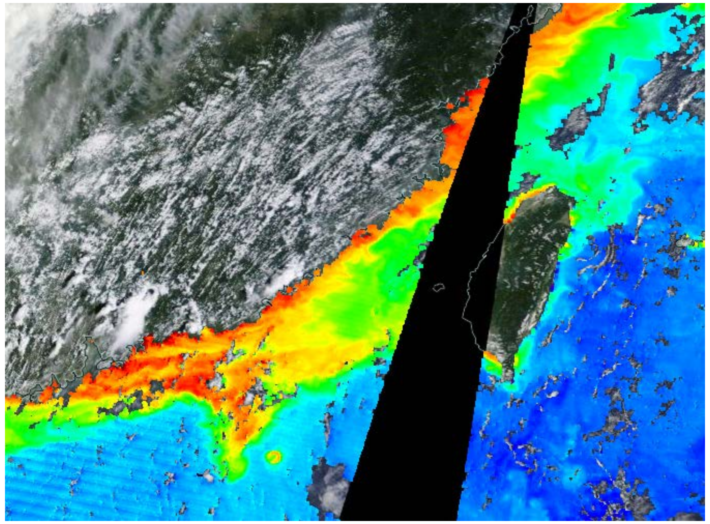

20 July 2016

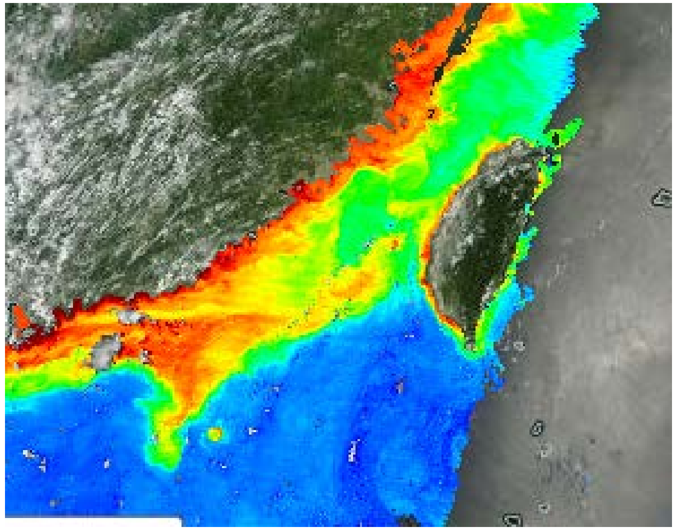

21 July 2016

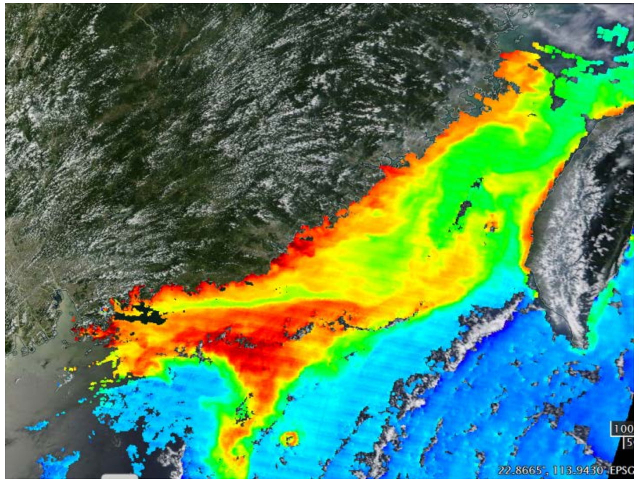

22 July 2016

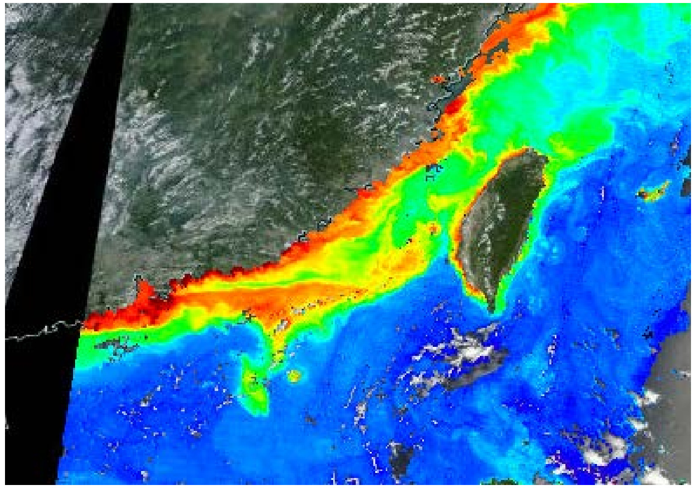

23 July 2016

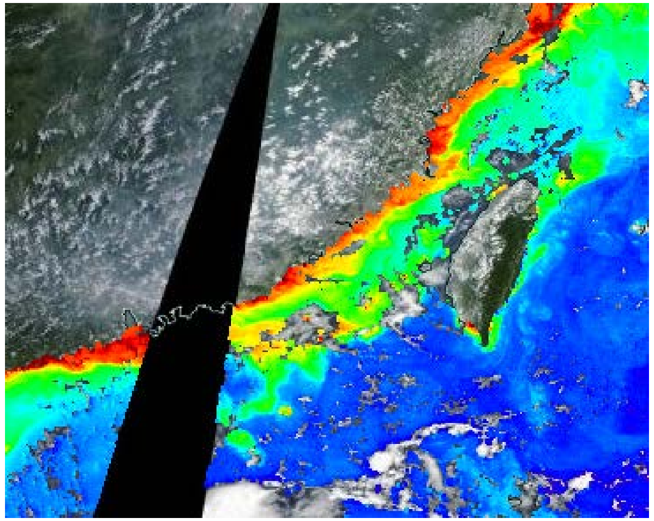

25 July 2016

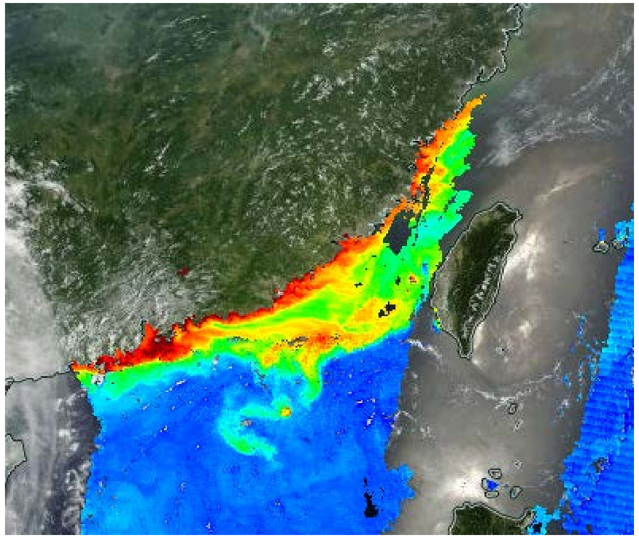

28 July 2016

Plans for the next years:

Carry out a more systematic investigation of the multiple sensor data showing the observed phenomena and gain a better understanding of the physical, chemical, and biological processes involved, in particular, by using numerical models.

Thank you for your attention